CARBON 97 (2016) 147–153

Contents lists available at ScienceDirect

CARBON

journal homepage: www.elsevier.com/locate/carbon

Chirality dependent corona phase molecular recognition of DNA-wrapped carbon nanotubes

Daniel P. Salem [a], Markita P. Landry [c], Gili Bisker [a], Jiyoung Ahn [a], Sebastian Kruss [b], Michael S. Strano [a,*]

[a] Department of Chemical Engineering, Massachusetts Institute of Technology, Cambridge, MA 02139, United States
[b] Institute for Physical Chemistry, Göttingen University, Germany
[c] Department of Chemical and Biomolecular Engineering, University of California, Berkeley, CA 94720, United States

ARTICLE INFO

Article history:
Received 10 July 2015
Received in revised form 19 August 2015
Accepted 22 August 2015
Available online 28 August 2015

ABSTRACT

Corona phase molecular recognition (CoPhMoRe) is a phenomenon whereby a polymer or surfactant corona phase wrapped around a nanoparticle selectively recognizes a particular molecule. The method can potentially generate non-biological, synthetic molecular recognition sites, analogous to antibodies, for a broad range of biomedical applications, including new types of sensors, laboratory and clinical assays, as well as inhibitors and targeted therapeutics. In this work, we utilize near infrared fluorescent single-walled carbon nanotubes (SWNTs) wrapped with specific single stranded DNA sequences to explore the (*n*,*m*) chirality dependence of CoPhMoRe. Specific DNA oligonucleotide sequences are known to recognize and interact uniquely with certain (*n*,*m*) SWNTs enabling their enrichment in ion exchange chromatography. We explore the CoPhMoRe effect using corona phases constructed from a library of 24 such sequences, screening against a biomolecule panel that includes common neurotransmitters, amino acids, saccharides and riboflavin. Example sequences include $(ATT)_4$, $(TAT)_4$ and $(ATTT)_3$ which recognize (7,5), (6,5) and (8,4) SWNTs, respectively. We find that these recognition sequences indeed form CoPhMoRe phases that are distinct among SWNT chiralities, and appear to pack more densely as to exclude analyte adsorption on the chirality they recognize. These results have encouraging implications for the controlled design of CoPhMoRe phases for biomedical applications.

1. Introduction

The polymer corona phase of individually-dispersed single-walled carbon nanotubes (SWNTs) forms the basis of many active areas of investigation including SWNT separation technologies [1,2], targeted biomolecule delivery [3,4], molecular detection [5], materials development and energy applications [6]. The inherent fluorescence of semiconducting single-walled carbon nanotubes has prompted their widespread use as signal transducers for optical sensing applications [7–9]. Their nearly indefinite fluorescence profile provides a significant advantage over conventional fluorophore-based detection platforms that are susceptible to photobleaching [10], and the overlap of their near infrared (nIR) fluorescence profile with the tissue transparency window makes them especially useful for in vivo applications [11–15]. These properties, along with the capability of single molecule detection [16], have made SWNT nanosensors valuable tools to study physical, chemical and biological processes at short length and time scales otherwise not obtainable from other detection platforms. As a result, considerable effort has been devoted to the design and development of SWNT-based optical sensors for a variety of target analytes including neurotransmitters [17], proteins [18–20], carbohydrates [21–23] and assorted small molecules [5,16,24].

Corona phase molecular recognition (CoPhMoRe) is a phenomenon whereby a heteropolymer or surfactant phase encapsulating a nanoparticle (i.e., a corona phase) recognizes a specific set of analytes as a result of the 3D structure displayed on the particle surface. Individually-dispersed semiconducting SWNTs have advantages for the discovery and utilization of such CoPhMoRe phases due to their nIR fluorescent response to molecular adsorption [7–9]. The study of CoPhMoRe phases is important for their ability to potentially generate non-biological, synthetic antibodies that may benefit a broad range of biomedical applications, including new types of sensors, laboratory and clinical assays, as well as inhibitors and targeted therapeutics [25]. To date, direct control over the design of such phases remains elusive. However, recent work in our lab has made progress in defining and addressing the CoPhMoRe inverse design problem for the rational design of a helically wrapping heteropolymer, which renders the underlying SWNT a sensor for an analyte of interest [26].

* Corresponding author.
E-mail address: strano@mit.edu (M.S. Strano).

http://dx.doi.org/10.1016/j.carbon.2015.08.075
0008-6223/

The effects of ssDNA length and sequence identity on recognition ability of a DNA–SWNT hybrid have not been thoroughly explored [27]. However, the impact of sequence length and composition on the strength and conformation of binding to SWNTs have been the focus of numerous studies [28–34]. In particular, Tu and coworkers identified specific DNA oligonucleotide sequences known to recognize and interact uniquely with certain (*n*,*m*) SWNTs enabling their enrichment in ion exchange chromatography [35]. Follow-up studies investigated the structure and binding strength of select recognition sequences and concluded that the sequences were able to bind more tightly to their respective chirality partners than to other chiralities [31,33,34].

In this work, we investigate the chirality dependent fluorescence modulation of DNA-wrapped SWNT sensors to a biomolecule panel that includes common neurotransmitters, amino acids, saccharides and riboflavin, in an effort to address the problem of CoPhMoRe design. We find that several recognition sequences indeed form CoPhMoRe phases that are distinct among SWNT chiralities and appear to pack more densely as to exclude analyte adsorption on the (*n*,*m*) chirality they recognize. Our study is the first effort to address chirality dependent CoPhMoRe, which establishes the framework for future applications including multiplexed analyte detection and ratiometric sensing for biomedical sensing and therapeutic applications.

2. Experimental

2.1. Materials

All chemicals were purchased from Sigma–Aldrich (USA) unless specified otherwise. All ssDNA sequences were purchased from IDT (USA). HiPco-SWNTs were purchased from Unidym (lot R1831) and processed according to the manufacturer's recommendation to remove residual impurities.

2.2. Suspension and characterization of ssDNA-wrapped SWNTs

HiPco-SWNTs were suspended in a 100 mM NaCl solution containing twice as much ssDNA by mass. Nanotubes were suspended using a 24-probe tip sonicator (Qsonica Q700) containing 3 mm probe tips and operating at a power of 96 W (4 W per sample) for 10 min, while in a cooling block. After sonication, each mixture was centrifuged twice at 16,000*g* for 90 min to remove SWNT aggregates and residual solid impurities. The supernatant was collected and characterized via ultraviolet (UV)–visible-nIR absorbance spectroscopy (Cary 5000, Agilent Technologies) to determine the concentration of each SWNT suspension [19]. Suspended SWNTs were stored at 4 °C to mitigate aggregation.

2.3. Near infrared fluorescence measurements

The fluorescence spectrum of each SWNT suspension was measured before and after the addition of an analyte. Prior to these measurements, SWNT solutions were diluted to a concentration of 1 mg/L using phosphate-buffered saline (PBS, pH = 7.4, 1×). Aliquots of 198 μL were added in triplicate to a 96-well plate (Tissue Culture Plates, Olympus Plastics) and allowed to equilibrate for at least 45 min. Samples were excited by a 785 nm laser (450 mW) using a Zeiss AxioVision inverted microscope and a 20× objective. Fluorescence was measured using a PI Acton SP2500 spectrometer and a Princeton Instruments InGaAs OMA V array detector. The 96-well plate was attached to an automated motorized stage above the objective to allow for high-throughput data collection. An exposure time of one second was used for all wrappings and the spectrum of each sample was background-corrected using a spectrum of PBS in an equivalent volume. The fluorescence spectrum of each sample was measured immediately after the addition of 2 μL of 10 mM analyte solution in PBS, resulting in a final analyte concentration of 100 μM. All analyte solutions were prepared immediately before addition to the sample wells.

2.4. Spectrum deconvolution

Fluorescence spectra were deconvoluted using a modified Matlab script developed previously by the Strano group (described in detail in the Supporting information of Ref. [5]). Normalized fluorescence responses were calculated for each chirality upon the addition of each analyte using the peak areas output by the deconvolution code.

3. Results and discussion

The ssDNA sequences used in this study are presented in Table 1, along with the chirality specificity of each sequence during ion exchange chromatography (if applicable) as determined by Tu and coworkers [35]. Nineteen sequences exhibiting chirality specificity were chosen, encompassing a variety of nanotube chiralities and diameters (1–19, Table 1). Five additional sequences of varying length and structure were also investigated in this study (20–24, Table 1). The absorbance spectra of all 24 sequences are provided in the Supplementary data (Fig. S1).

Each fluorescence emission spectrum was processed by a deconvolution Matlab script to isolate the fluorescence contributions of individual chiralities (Fig. 1a). Since the (9,4) and (7,6) peaks are largely overlapping, we tracked the peak area values when calculating the fluorescence response of each chirality and combined the peak areas of the (9,4) and (7,6) peaks to avoid potential artifacts introduced by the fitting algorithm during the deconvolution. The 24 ssDNA wrappings were screened against nine different analytes (Fig. 1b), several of which were previously shown to induce strong sensor responses for DNA-wrapped nanotubes [5,17]. Glucose and sucrose were added to the sensors at a concentration of 10 mM, which resembles the glucose concentration in human blood. Moreover, riboflavin was added at a concentration of 1 μM due to its limited solubility in PBS.

As expected, all three catecholamines (dopamine, epinephrine, and norepinephrine) as well as ascorbic acid induced similar, strong turn-on responses across nearly all of the sensor wrappings tested. While each DNA-SWNT hybrid exhibited some degree of variability in the response of each chirality, as demonstrated for the $(GT)_{15}$-SWNT data in Fig. 2, most wrappings did not exhibit systematic chirality dependence attributable to their recognition abilities during ion exchange chromatography (Supplementary Fig. S2). However, as shown in Fig. 2, the sequences $(TAT)_4$ and $(ATTT)_3$ did exhibit chirality dependent responses that appear to correlate well with their reported chirality specificities of (6,5) and (8,4) respectively. Although the (8,4) chirality was not included in the deconvolution algorithm, the (9,4) and (7,6) chiralities, which emit at roughly the same wavelength as (8,4) SWNT, are nearly unresponsive to the addition of dopamine and other catecholamines (Supplementary Figs. S4 and S5). Additionally, the smaller diameter SWNTs for the $(TAT)_4$ wrapping, particularly the (6,5) chirality, were much less responsive than larger diameter chiralities including (12,1) and (11,3).

The chirality dependence observed following dopamine addition (Fig. 2) was consistent for other analytes in this study. Fig. 3 presents the chirality dependent sensor responses to 100 μM epinephrine, 100 μM norepinephrine and 1 μM riboflavin. Consistent with the catecholamine results, the (9,4) and (7,6) chiralities of $(ATTT)_3$-wrapped SWNTs were nearly unresponsive to riboflavin,

Table 1
List of ssDNA wrappings tested in this study. $(EG)_6$ is a hexa-ethyleneglycol spacer.

Sequence number	ssDNA sequence	Chirality specificity*	Sequence number	ssDNA sequence	Chirality specificity*
1	$(TCC)_{10}$	(9,1)	13	$(GT)_6$	(8,6)
2	$(TGA)_{10}$	(9,1)	14	$(GTC)_3$	(8,6)
3	$(TTA)_4TT$	(8,3)	15	$(TATT)_3T$	(8,6)
4	$(TAT)_4$	(6,5)	16	$(GTC)_2$	(8,6)
5	$(CGT)_3C$	(6,5)	17	$(TCG)_2TC$	(8,6)
6	$(ATT)_4$	(7,5)	18	$(TGTT)_2TGT$	(9,5)
7	$(TATT)_2TAT$	(10,2)	19	$(CCG)_2CC$	(8,7)
8	$(ATTT)_3$	(8,4)	20	$(TTA)_3T$	–
9	$(GTC)_2GT$	(9,4)	21	$(GU)_5$	–
10	$(CCG)_4$	(9,4)	22	$(GT)_8$-$((EG)_6)_5$-$(GT)_7$	–
11	$(GTT)_3G$	(7,6)	23	$(GT)_{15}$	–
12	$(TGT)_4T$	(7,6)	24	$(GA)_{15}$	–

* Ref. [35].

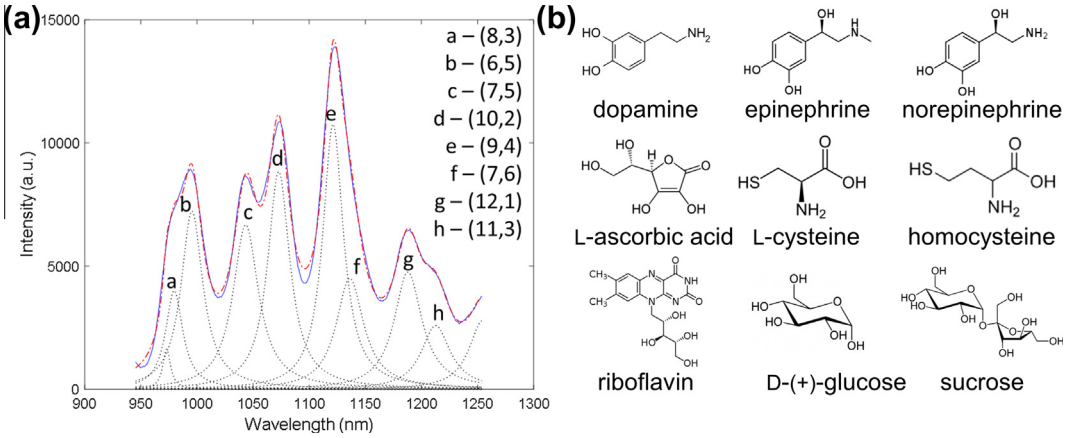

Fig. 1. (a) Deconvolution of a fluorescence spectrum of $(GT)_{15}$-wrapped SWNT: original spectrum (blue curve), individual chirality contributions (dashed black curves) and the sum of the individual peaks (dashed red curve). (b) Small molecule analytes used in this study. Dopamine, epinephrine, norepinephrine and ascorbic acid have been reported to elicit turn-on responses for DNA-wrapped SWNTs [17], while riboflavin was previously reported to quench fluorescence for $(GT)_{15}$-wrapped SWNTs [5]. (For interpretation of the references to color in this figure legend, the reader is referred to the web version of this article.)

exhibiting a 5% decrease in fluorescence compared to a 40% decrease exhibited by $(GT)_{15}$-wrapped SWNTs (Supplementary Fig. S6) and a 30% decrease exhibited by $(TAT)_4$-wrapped SWNTs. Analogous plots for the remaining analytes contain the same trends as Fig. 3 and are provided in the Supplementary data. The detection limits for $(TAT)_4$- and $(ATTT)_3$-wrapped SWNTs were determined for epinephrine by measuring the sensor responses to different concentrations of analyte and constructing a calibration curve for each chirality (Fig. S8). Each limit of detection was calculated as the concentration on the calibration curve corresponding to the sum of the mean control response (just PBS buffer) and three times the standard deviation. While there was a small degree of variability in the detection limits among different chiralities, $(TAT)_4$- and $(ATTT)_3$-wrapped SWNTs exhibited average detection limits of 20 and 11 nM, respectively.

To ensure that the chirality dependent sensor responses were triggered by analyte – SWNT interaction rather than by polymer wrapping rearrangement while equilibrating in solution, we monitored the fluorescence emission over a period of 4 h after dilution to 1 mg/L. Recently, Landry et al. reported that RNA-wrapped SWNTs slowly equilibrated upon dilution in PBS, as manifested by a gradual fluorescence modulation over several hours [36], whereas DNA wrappings showed a much more stable fluorescence signal after dilution. Although 23 of the 24 sequences used in this study were DNA, many sequences were much shorter than the 30-mer oligonucleotides used in the previous work and may not bind as tightly. To rule out equilibration artifacts, the fluorescence spectra of $(GT)_{15}$-, $(TAT)_4$- and $(ATTT)_3$-wrapped SWNTs were collected every 10 min for 4 h after dilution to 1 mg/L with PBS, and were then deconvoluted and inspected for chirality dependent stability. We found that the oligonucleotide wrappings were remarkably stable after PBS dilution over the course of the experiment, demonstrated by an invariant fluorescent emission signal over time (see Supplementary Fig. S9).

The use of 785 nm laser excitation for the nIR fluorescence experiments did not allow us to isolate the fluorescence contribution of (8,4) SWNTs ($(ATTT)_3$ recognition partner), which fluoresce more strongly at shorter excitation wavelengths. To address this problem and better visualize the fluorescence responses of each chirality, we measured the excitation/emission profiles for $(TAT)_4$- and $(ATTT)_3$-wrapped SWNTs before and after the addition of 100 μM ascorbic acid. These experiments were completed using a custom-built setup containing a xenon arc lamp and an Acton SpectraPro 2150i monochromator. The SWNT samples were excited at wavelengths between 475 and 775 nm in intervals of 5 nm and the data were processed to account for the variation in the power profile of the xenon lamp. The excitation wavelengths were calibrated using a known standard. Fig. 4 provides the resulting photoluminescence maps of both ssDNA-SWNT conjugates. As expected, $(TAT)_4$-wrapped (6,5) SWNTs did not exhibit a strong response to 100 μM ascorbic acid, in contrast to larger diameter SWNTs including (8,4), (7,6), (10,2) and (9,4). Moreover, $(ATTT)_3$-wrapped (8,4) and (9,4) SWNTs did not respond strongly to ascorbic acid, while other SWNT chiralities—including (7,6)—did exhibit a response. These data further support our earlier results of chirality-dependent CoPhMoRe, and in particular, our findings that the $(TAT)_4$ and $(ATTT)_3$ ssDNA wrappings induce a reduction in sensor responsivity for their respective chirality partners.

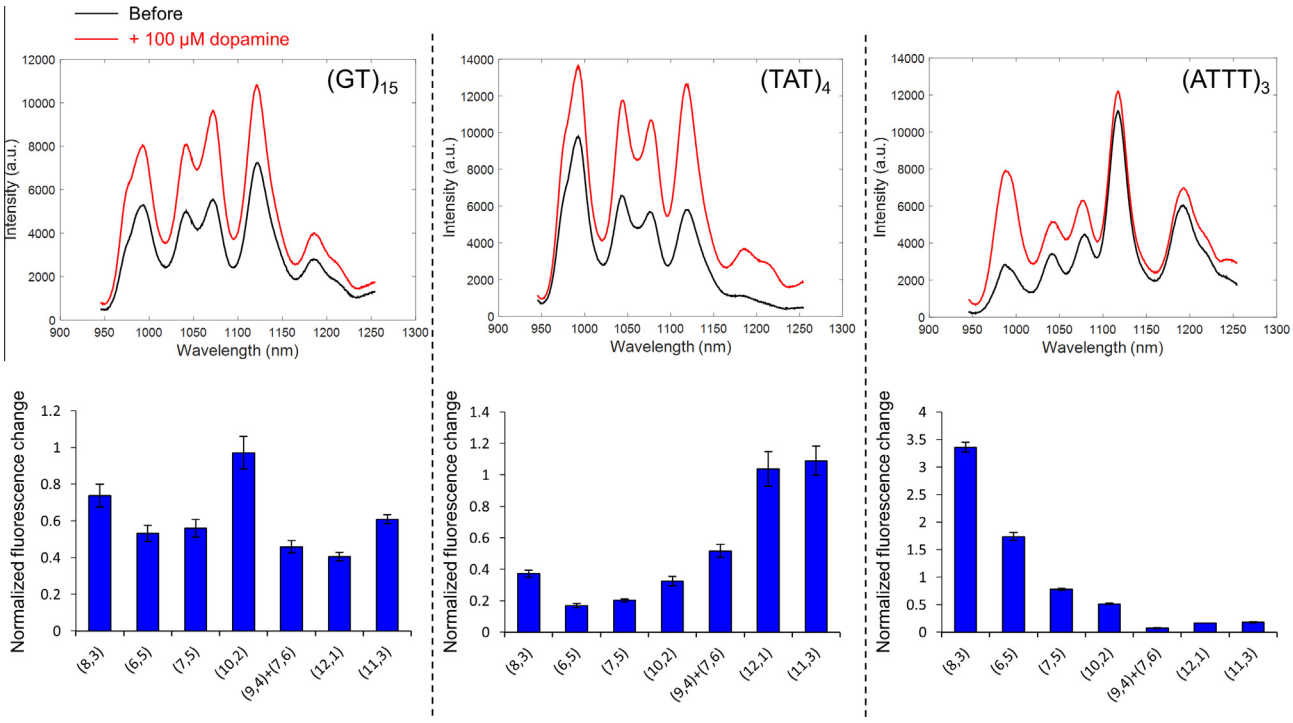

Fig. 2. Fluorescence spectra before (black) and after (red) the addition of 100 μM dopamine for the wrappings $(GT)_{15}$, $(TAT)_4$ and $(ATTT)_3$ as well as the normalized fluorescence response of each chirality. (For interpretation of the references to color in this figure legend, the reader is referred to the web version of this article.)

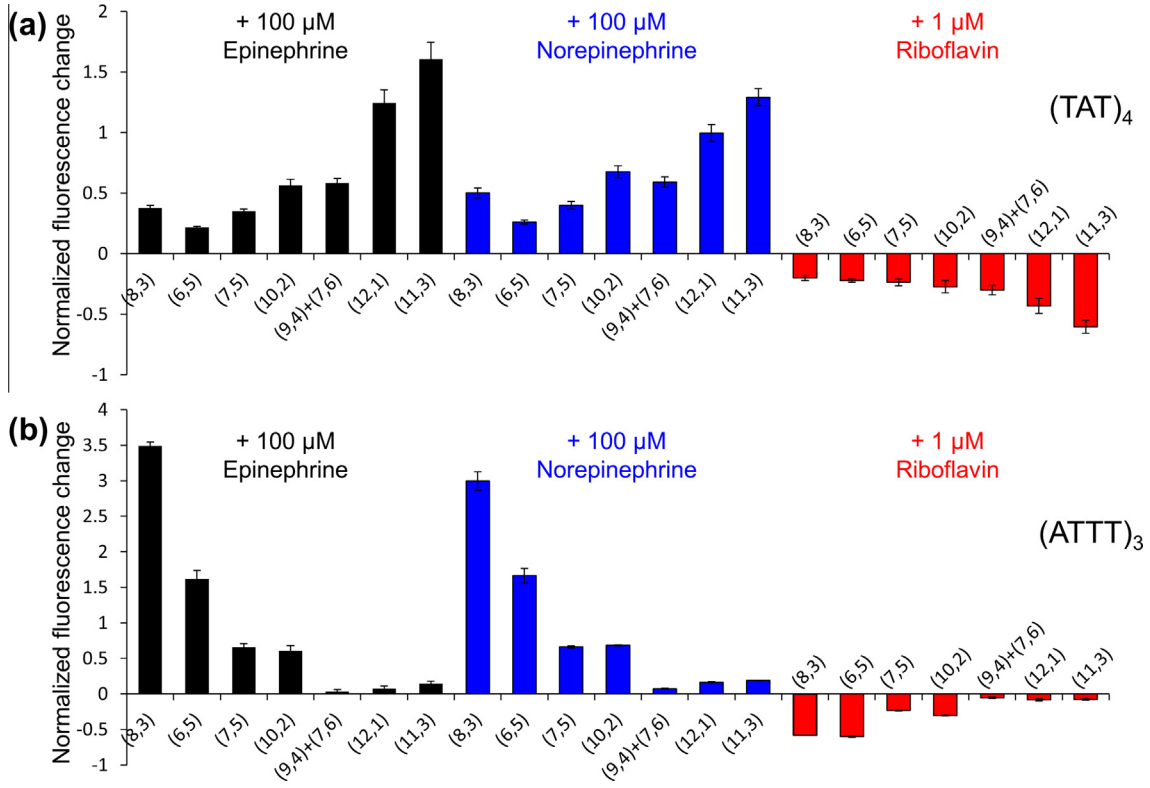

Fig. 3. Chirality dependent responses of (a) $(TAT)_4$-wrapped and (b) $(ATTT)_3$-wrapped SWNTs upon the addition of 100 μM epinephrine (black), 100 μM norepinephrine (blue) and 1 μM riboflavin (red). (For interpretation of the references to color in this figure legend, the reader is referred to the web version of this article.)

For a molecule to induce a sensor response, it must be able to access the nanotube surface and displace a portion of the DNA wrapping, as demonstrated by Kruss et al. using SWNTs wrapped with Cy3-labeled DNA [17]. When adsorbed onto the SWNT surface, the Cy3 dye is completely quenched; however, upon the addition of dopamine, Kruss et al. reported a restoration of the Cy3

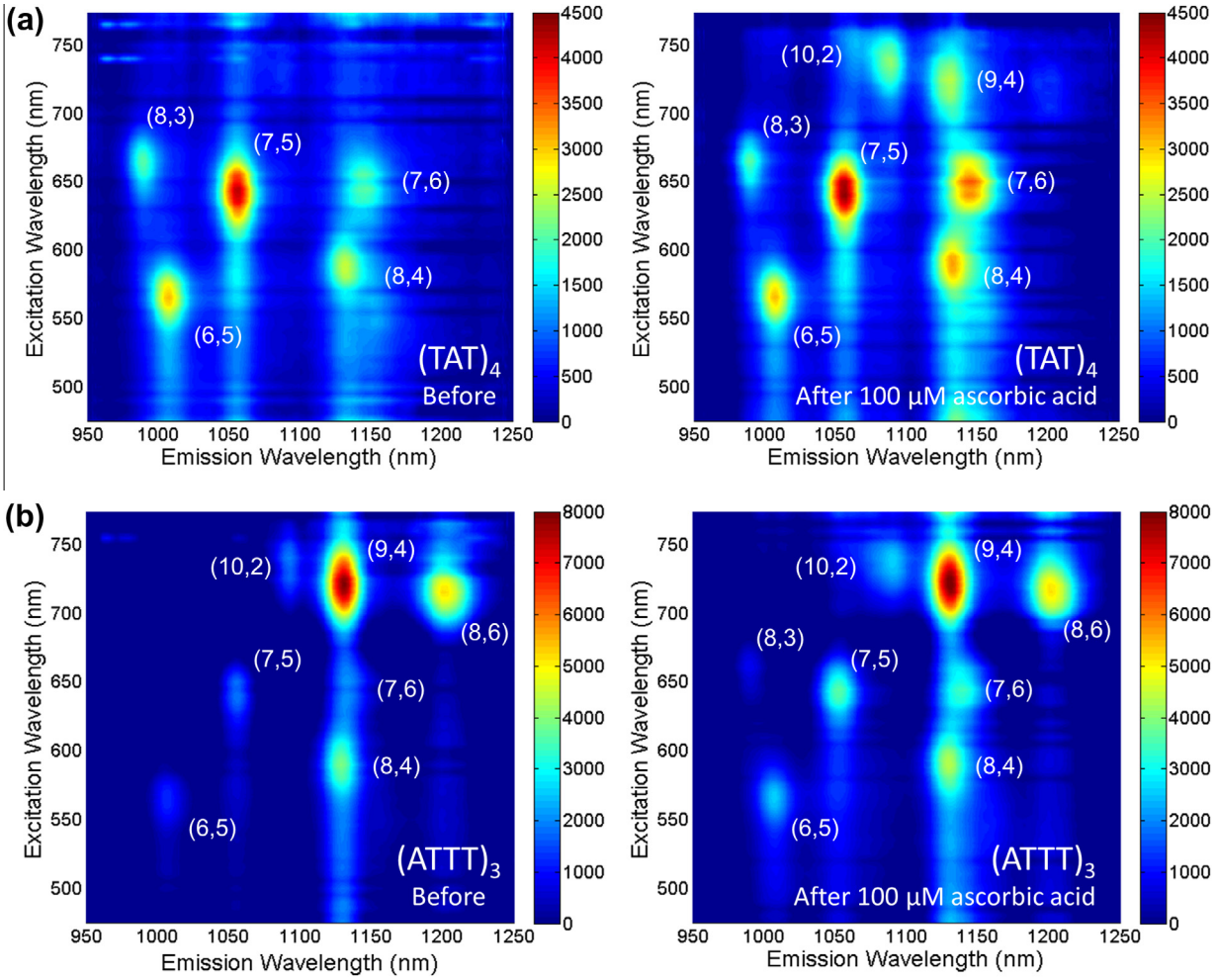

Fig. 4. Excitation-emission profiles for (a) $(TAT)_4$-wrapped and (b) $(ATTT)_3$-wrapped SWNTs before and after the addition of 100 µM ascorbic acid. Spectra were collected in intervals of 5 nm using exposure times of 5 min. for the $(TAT)_4$-SWNTs and 5.5 min. for the $(ATTT)_3$-SWNTs. (For interpretation of the references to color in this figure legend, the reader is referred to the web version of this article.)

fluorescence, indicating the desorption of the Cy3 from the nanotube surface. Thus, the chirality dependence observed in this study can be explained by corona structure variability—and hence, variability in analyte accessibility to the SWNT surface—across different chiralities for the same ssDNA wrapping. Molecular dynamics simulations have been extensively used to study the corona architecture of DNA-SWNT hybrids and a combination of molecular dynamics and surfactant exchange experiments have shown that corona architecture and binding strength vary across different chiralities for several sequences exhibiting separation capability including $(TAT)_4$ [32–34]. Both corona structure and binding strength are dependent on a combination of nanotube diameter and electronic properties, which can be clearly observed in the chirality dependent responses of $(TAT)_4$-wrapped SWNTs. While smaller diameter nanotubes, in general, exhibited attenuated responsivity, the (6,5) chirality consistently responded the least for all analytes tested. Given the chirality dependent response trends observed for both $(TAT)_4$ and $(ATTT)_3$, it is likely that the chiralities exhibiting weaker sensor responses contain more tightly-packed corona phases. The ability of these sequences to exhibit stronger chirality dependence than the other recognition sequences tested could be caused by an increased sensitivity of binding strength on SWNT chirality. This phenomenon was previously reported for the sequences $(TAT)_4$, $(CCA)_{10}$ and $(TTA)_4TT$, where surfactant exchange experiments indicated that the difference in binding strength across various chiralities was much larger for $(TAT)_4$ than for the other sequences [34].

With the growing interest in utilizing fluorescent SWNTs as biomedical sensors capable of label free analyte detection [25], single chirality sensors would be extremely valuable for many applications. Owing to the unique emission wavelength associated with each chirality, multiple targets can be detected simultaneously by hyperspectral imaging techniques. Such capabilities open up new possibilities in the biomedical field by allowing researchers to study complex biological processes by monitoring several important bio-markers at the same time, using selective sensors with different chiralities. SWNT sensors were utilized for monitoring nitric oxide in vivo [13], vitamin dynamics within cells [5], and protein–protein interactions [18]. In addition to multiplexed detection and improved signal to noise ratio, chirality specific sensors would allow for an internal fluorescent standard that would eliminate the need for signal calibration or allow for ratiometric sensing. This was recently demonstrated for the detection of nitric oxide and hydrogen peroxide within living plants [37]. Moreover, chirality dependent CoPhMoRe may be particularly useful in distinguishing between closely related analyte molecules which tend to induce similar sensor responses. A variation in chirality dependent responses induced by two or more structurally similar molecules will allow for their selective detection by utilizing the responses of several chiralities. Such a strategy may be needed to design

SWNT sensors that can effectively discriminate between structurally similar carbohydrate molecules or between various catecholamines and ascorbic acid, both of which remain subjects of ongoing studies [38–41].

4. Conclusions

The recent emergence of optical detection methods for molecular recognition has spurred interest in understanding the parameters which contribute to molecular specificity and selectivity. Based on a previous study reporting ssDNA sequences capable of separating single chirality SWNTs from a mixture during ion exchange chromatography, we examined the effect of such sequences on SWNT fluorescence and molecular recognition. In particular, we studied the chirality dependent photoluminescence responses of polynucleotide-wrapped SWNT to a library of relevant biomolecules including catecholamines, carbohydrates and amino acids. The experimental results identified two particular ssDNA sequences, $(TAT)_4$ and $(ATTT)_3$, that formed DNA-SWNT hybrids exhibiting significant chirality dependent fluorescence responses to all of the analytes tested. The observed chirality dependence was consistent with previously reported results indicating that the ssDNA sequences capable of single chirality separation are more tightly bound to their respective chirality partners. Our results open up a new path towards single chirality SWNT sensors allowing for multiplexed and ratiometric label-free detection of multiple biomolecules for biomedical research and applications. Moreover, our work motivates the continuous search for antibody analogs for molecular recognition as well as the optimization of currently available optical nanosensors using novel nanoscience and nanotechnology tools.

Acknowledgements

We gratefully acknowledge discussions with Strano group members regarding this manuscript. D.P.S. is grateful for a National Science Foundation Graduate Research Fellowship under Grant No. 2388357. M.P.L. acknowledges an NSF postdoctoral research fellowship under Award No. 1306229, a Burroughs Wellcome Fund Career Award at the Scientific Interface (CASI) and a NARSAD Young Investigator Award. M.S.S acknowledges support by the National Science Foundation under award number 1213622, and the Juvenile Diabetes Research Foundation.

Appendix A. Supplementary data

Supplementary data associated with this article can be found, in the online version, at http://dx.doi.org/10.1016/j.carbon.2015.08.075.

References

[1] M.S. Arnold, A.A. Green, J.F. Hulvat, S.I. Stupp, M.C. Hersam, Sorting carbon nanotubes by electronic structure using density differentiation, Nat. Nanotechnol. 1 (1) (2006) 60–65.
[2] M. Zheng, A. Jagota, E.D. Semke, B.A. Diner, R.S. Mclean, S.R. Lustig, et al., DNA-assisted dispersion and separation of carbon nanotubes, Nat. Mater. 2 (5) (2003) 338–342.
[3] A. Karmakar, S.M. Bratton, E. Dervishi, A. Ghosh, M. Mahmood, Y. Xu, et al., Ethylenediamine functionalized-single-walled nanotube (f-SWNT)-assisted in vitro delivery of the oncogene suppressor p53 gene to breast cancer MCF-7 cells, Int. J. Nanomed. 6 (2011) 1045–1055.
[4] J.P. Giraldo, M.P. Landry, S.M. Faltermeier, T.P. McNicholas, N.M. Iverson, A.A. Boghossian, et al., Plant nanobionics approach to augment photosynthesis and biochemical sensing (vol 13, pg 400, 2014), Nat. Mater. 13 (5) (2014) 530.
[5] J.Q. Zhang, M.P. Landry, P.W. Barone, J.H. Kim, S.C. Lin, Z.W. Ulissi, et al., Molecular recognition using corona phase complexes made of synthetic polymers adsorbed on carbon nanotubes, Nat. Nanotechnol. 8 (12) (2013) 959–968.
[6] Q.H. Wang, D.O. Bellisario, L.W. Drahushuk, R.M. Jain, S. Kruss, M.P. Landry, et al., Low dimensional carbon materials for applications in mass and energy transport, Chem. Mater. 26 (1) (2014) 172–183.
[7] M.J. O'Connell, S.M. Bachilo, C.B. Huffman, V.C. Moore, M.S. Strano, E.H. Haroz, et al., Band gap fluorescence from individual single-walled carbon nanotubes, Science 297 (5581) (2002) 593–596.
[8] S.M. Bachilo, M.S. Strano, C. Kittrell, R.H. Hauge, R.E. Smalley, R.B. Weisman, Structure-assigned optical spectra of single-walled carbon nanotubes, Science 298 (5602) (2002) 2361–2366.
[9] P.W. Barone, S. Baik, D.A. Heller, M.S. Strano, Near-infrared optical sensors based on single-walled carbon nanotubes, Nat. Mater. 4 (1) (2005). 86–U16.
[10] D.A. Heller, S. Baik, T.E. Eurell, M.S. Strano, Single-walled carbon nanotube spectroscopy in live cells: towards long-term labels and optical sensors, Adv. Mater. 17 (23) (2005). 2793–+.
[11] K. Welsher, S.P. Sherlock, H.J. Dai, Deep-tissue anatomical imaging of mice using carbon nanotube fluorophores in the second near-infrared window, Proc. Natl. Acad. Sci. USA 108 (22) (2011) 8943–8948.
[12] A.A. Boghossian, J.Q. Zhang, P.W. Barone, N.F. Reuel, J.H. Kim, D.A. Heller, et al., Near-infrared fluorescent sensors based on single-walled carbon nanotubes for life sciences applications, Chemsuschem 4 (7) (2011) 848–863.
[13] N.M. Iverson, P.W. Barone, M. Shandell, L.J. Trudel, S. Sen, F. Sen, et al., In vivo biosensing via tissue-localizable near-infrared-fluorescent single-walled carbon nanotubes, Nat. Nanotechnol. 8 (11) (2013) 873–880.
[14] G.S. Hong, S. Diao, J.L. Chang, A.L. Antaris, C.X. Chen, B. Zhang, et al., Through-skull fluorescence imaging of the brain in a new near-infrared window, Nat. Photonics 8 (9) (2014) 723–730.
[15] G. Bisker, N.M. Iverson, J. Ahn, M.S. Strano, A pharmacokinetic model of a tissue implantable insulin sensor, Adv. Healthcare Mater. 4 (1) (2015) 87–97.
[16] J.Q. Zhang, A.A. Boghossian, P.W. Barone, A. Rwei, J.H. Kim, D.H. Lin, et al., Single molecule detection of nitric oxide enabled by d(AT)(15) DNA adsorbed to near infrared fluorescent single-walled carbon nanotubes, J. Am. Chem. Soc. 133 (3) (2011) 567–581.
[17] S. Kruss, M.P. Landry, E. Vander, B.M.A. Lima, N.F. Reuel, J.Q. Zhang, et al., Neurotransmitter detection using corona phase molecular recognition on fluorescent single-walled carbon nanotube sensors, J. Am. Chem. Soc. 136 (2) (2014) 713–724.
[18] J.H. Ahn, J.H. Kim, N.F. Reuel, P.W. Barone, A.A. Boghossian, J.Q. Zhang, et al., Label-free, single protein detection on a near-infrared fluorescent single-walled carbon nanotube/protein microarray fabricated by cell-free synthesis, Nano Lett. 11 (7) (2011) 2743–2752.
[19] J.Q. Zhang, S. Kruss, A.J. Hilmer, S. Shimizu, Z. Schmois, F. De La Cruz, et al., A rapid, direct, quantitative, and label-free detector of cardiac biomarker troponin T using near-infrared fluorescent single-walled carbon nanotube sensors, Adv. Healthcare Mater. 3 (3) (2014) 412–423.
[20] J.T. Nelson, S. Kim, N.F. Reuel, D.P. Salem, G. Bisker, M.P. Landry, et al., The mechanism of immobilized protein A binding to IgG on nanosensor array surfaces, Anal. Chem. 87 (16) (2015) 8186–8193.
[21] P.W. Barone, R.S. Parker, M.S. Strano, In vivo fluorescence detection of glucose using a single-walled carbon nanotube optical sensor: design, fluorophore properties, advantages, and disadvantages, Anal. Chem. 77 (23) (2005) 7556–7562.
[22] B. Mu, J. Ahn, T.P. McNicholas, M.S. Strano, Generating selective saccharide binding affinity of phenyl boronic acids by using single-walled carbon nanotube corona phases, Chem.-A Eur. J. 21 (12) (2015) 4523–4528.
[23] N.F. Reuel, J.H. Ahn, J.H. Kim, J.Q. Zhang, A.A. Boghossian, L.K. Mahal, et al., Transduction of glycan-lectin binding using near-infrared fluorescent single-walled carbon nanotubes for glycan profiling, J. Am. Chem. Soc. 133 (44) (2011) 17923–17933.
[24] H. Jin, D.A. Heller, M. Kalbacova, J.H. Kim, J.Q. Zhang, A.A. Boghossian, et al., Detection of single-molecule H_2O_2 signalling from epidermal growth factor receptor using fluorescent single-walled carbon nanotubes, Nat. Nanotechnol. 5 (4) (2010). 302-U81..
[25] S. Kruss, A.J. Hilmer, J. Zhang, N.F. Reuel, B. Mu, M.S. Strano, Carbon nanotubes as optical biomedical sensors, Adv. Drug Deliv. Rev. 65 (15) (2013) 1933–1950.
[26] G. Bisker, J. Ahn, S. Kruss, Z.W. Ulissi, D.P. Salem, M.S. Strano, A mathematical formulation and solution of the CoPhMoRe inverse problem for helically wrapping polymer corona phases on cylindrical substrates, J. Phys. Chem. C 119 (24) (2015) 13876–13886.
[27] M.P. Landry, S. Kruss, J.T. Nelson, G. Bisker, N.M. Iverson, N.F. Reuel, et al., Experimental tools to study molecular recognition within the nanoparticle corona, Sensors 14 (9) (2014) 16196–16211.
[28] F. Albertorio, M.E. Hughes, J.A. Golovchenko, D. Branton, Base dependent DNA–carbon nanotube interactions: activation enthalpies and assembly–disassembly control, Nanotechnology 20 (39) (2009).
[29] R.R. Johnson, A.T.C. Johnson, M.L. Klein, Probing the structure of DNA–carbon nanotube hybrids with molecular dynamics, Nano Lett. 8 (1) (2008) 69–75.
[30] S. Manohar, T. Tang, A. Jagota, Structure of homopolymer DNA–CNT hybrids, J. Phys. Chem. C 111 (48) (2007) 17835–17845.
[31] D. Roxbury, A. Jagota, J. Mittal, Sequence-specific self-stitching motif of short single-stranded DNA on a single-walled carbon nanotube, J. Am. Chem. Soc. 133 (34) (2011) 13545–13550.
[32] D. Roxbury, A. Jagota, J. Mittal, Structural characteristics of oligomeric DNA strands adsorbed onto single-walled carbon nanotubes, J. Phys. Chem. B 117 (1) (2013) 132–140.
[33] D. Roxbury, X.M. Tu, M. Zheng, A. Jagota, Recognition ability of DNA for carbon nanotubes correlates with their binding affinity, Langmuir 27 (13) (2011) 8282–8293.

[34] A. Shankar, J. Mittal, A. Jagota, Binding between DNA and carbon nanotubes strongly depends upon sequence and chirality, Langmuir 30 (11) (2014) 3176–3183.
[35] X.M. Tu, S. Manohar, A. Jagota, M. Zheng, DNA sequence motifs for structure-specific recognition and separation of carbon nanotubes, Nature 460 (7252) (2009) 250–253.
[36] M.P. Landry, L. Vukovic, S. Kruss, G. Bisker, A.M. Landry, S. Islam, et al., Comparative dynamics and sequence dependence of DNA and RNA binding to single walled carbon nanotubes, J. Phys. Chem. C 119 (18) (2015) 10048–10058.
[37] J.P. Giraldo, M.P. Landry, S.Y. Kwak, R.M. Jain, M.H. Wong, N.M. Iverson, et al., A ratiometric sensor using single chirality near-infrared fluorescent carbon nanotubes: application to in vivo monitoring, Small (2015).
[38] H.X. Ju, X.J. Zhang, J. Wang, Carbohydrate detection using nanostructured biosensing, Nanobiosensing: Principles, Develop. Appl. (2011) 393–424.
[39] I. Mitra, Z.X. Zhuang, Y.N. Zhang, C.Y. Yu, Z.T. Hammoud, H.X. Tang, et al., *N*-glycan profiling by microchip electrophoresis to differentiate disease states related to esophageal adenocarcinoma, Anal. Chem. 84 (8) (2012) 3621–3627.
[40] J.J. Colleran, C.B. Breslin, Simultaneous electrochemical detection of the catecholamines and ascorbic acid at PEDOT/S-beta-CD modified gold electrodes, J. Electroanal. Chem. 667 (2012) 30–37.
[41] A. Chaicham, S. Sahasithiwat, T. Tuntulani, B. Tomapatanaget, Highly effective discrimination of catecholamine derivatives via FRET-on/off processes induced by the intermolecular assembly with two fluorescence sensors, Chem. Commun. 49 (81) (2013) 9287–9289.